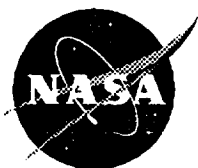NASA Technical Paper 3539

Rapid Mars Transits With Exhaust-Modulated Plasma Propulsion

Franklin R. Chang-Díaz
Michael M. Hsu
Ellen Braden
Ivan Johnson
Tien Fang Yang

March 1995

Rapid Mars Transits With Exhaust-Modulated Plasma Propulsion

Franklin R. Chang-Díaz, Ellen Braden, and Ivan Johnson
Lyndon B. Johnson Space Center
Houston, Texas

Michael M. Hsu
United States Navy
det. Department of Physics
Cambridge University, U.K.

Tien Fang Yang
Yang Technologies, Inc.
Cambridge, Massachusetts

Contents

Figures

Tables

Abstract

The operational characteristics of the Exhaust-Modulated Plasma Rocket are described. Four basic human and robotic mission scenarios to Mars are analyzed using numerical optimization techniques at variable specific impulse and constant power. The device is well-suited for "split-sprint" missions allowing fast, one-way low-payload human transits of 90 to 104 days, as well as slower, 180-day, high-payload robotic precursor flights. Abort capabilities, essential for human missions, are also explored.

1. Introduction

Notwithstanding the present emphasis on the assembly of a permanent space station in low Earth orbit, human missions to the planet Mars and beyond continue to captivate the imagination of scientists and engineers. Such missions embody the ultimate expression of human adventure and exploration. To be sure, steady, albeit limited, efforts to map out human exploration scenarios have continued.[1, 2, 3] These scenarios have stimulated many dormant technologies and helped integrate them into increasingly realistic vehicle propulsion concepts.

Two areas of special interest are space nuclear power and advanced (nonchemical) propulsion. Foreseeable developments in these areas will, nevertheless, still result in systems which are inherently power-limited. For example, in the development of advanced propulsion, the attainment of high exhaust-velocity or specific impulse (Isp) comes at the expense of vehicle thrust. Gains in rocket performance, measured as payload mass fraction, imply very long trip times. Conversely, short trip times result in very low-payload capability.

This unfortunate situation can be greatly alleviated by the continuous modulation of the rocket exhaust, permitting considerably shorter transit times with reasonable payload. This technology has now come of age with the development of plasma heating and magnetic confinement schemes for fusion research. These combinations have been successfully adapted to rocket propulsion and have resulted in a high-power density rocket which is also capable of continuous exhaust modulation at constant power.[4] The performance and capabilities of such a tunable plasma device are the subject of this paper.

2. Operational Modes

The concept of exhaust modulation has been known theoretically since the early 1950s.[5, 6, 7] Using this technique, maximum payload capability for a given trip time can be obtained through an optimum schedule that takes into account the local strength of the gravitational well in which the vehicle moves. Moreover, such systems are inherently flexible and provide the rocket with not only propulsion during the cruise phase, but also maneuvering capability upon reaching its destination. These systems also allow the implementation of a two-stage "split sprint" mission (see section 4) with the same rocket. One-way, 180-day nonhuman cargo missions with 66% payload can be achieved. At the same time, 90- to 100-day fast human missions with from 2 to 14% payload capacity are also possible.

Until the late 1960s, the technology to construct these systems had remained elusive. Nuclear-electric rockets suffering from limitations in power density due to electrode erosion focused on the achievement of high, fixed Isp. Chemical and nuclear-thermal rockets with fixed area nozzles, on the other hand, are incapable of thrust/Isp variation at constant power. In contrast, the present radio frequency (RF)-heated, magnetically vectored plasma design does not suffer from these limitations. In this type of rocket, exhaust parameters are mainly determined by input power and the confining properties of the magnetic field.

The utilization of magnetic nozzles alleviates the materials constraints which impose limits on exhaust temperature. Such rockets exhibit a wide operational range in two basic modes: a high thrust/low Isp initial profile, followed by a low thrust/high Isp one as the vehicle loses mass and escapes the gravitational well.

3. System Description

As described elsewhere,[8, 9, 10] the Variable Isp Plasma Rocket is an electrodeless, electrothermal, RF-heated plasma propulsion device capable of continuous thrust/Isp modulation at constant power. The system, shown in Fig.1, consists of three major magnetic cells, denoted as "forward," "central," and "aft," all of which are linked together to form an asymmetric tandem mirror machine.[11] The forward end-cell comprises the main injection and ionization subsystem; the central-cell serves as a power amplifier. The aft end-cell provides the flow vectoring and exhaust and ensures its efficient detachment from the magnetic field. The general system parameters are listed in Table 1.

Operationally, neutral gaseous fuel (typically hydrogen) is injected at the forward end-cell and ionized there by electron cyclotron resonance heating. This initial cold plasma is subsequently heated and controlled to the desired temperature and density by ion cyclotron resonance heating. The
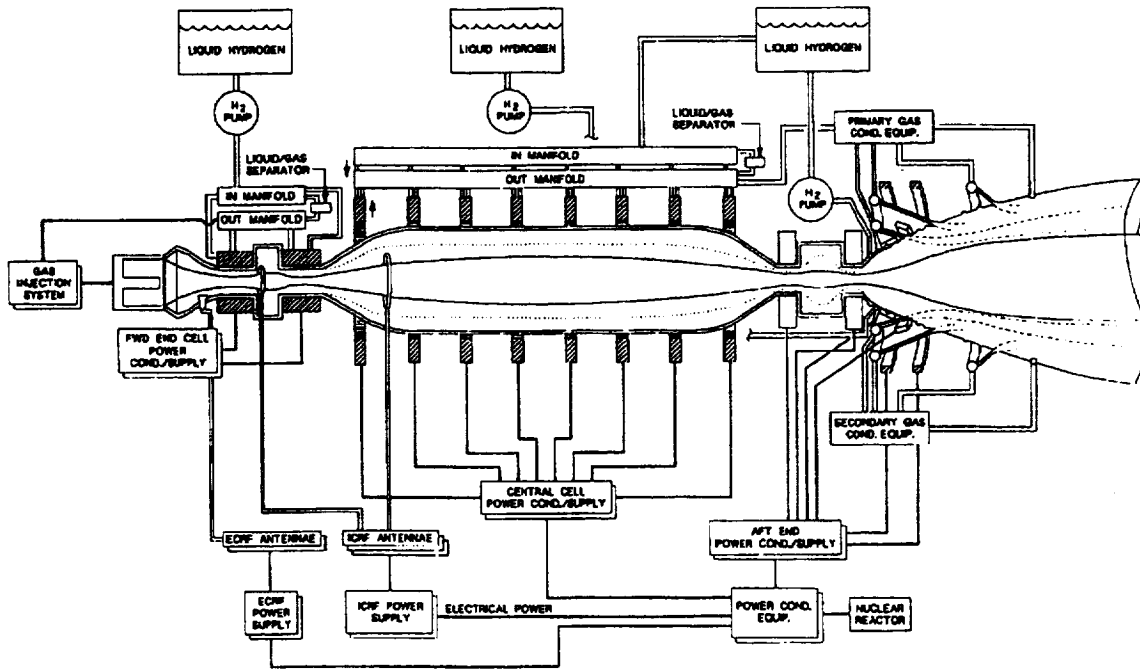
Figure 1. Schematic representation of the variable Isp (or exhaust-modulated) plasma rocket.

latter process occurs in the much larger central-cell of the device. After heating, the plasma enters a two-stage hybrid nozzle at the aft end-cell where it is exhausted to provide modulated thrust.

Table 1. General System Parameters

Variable frequency	500 kHz to 10 Mhz
Four double half loop antennae in central-cell	2 MW - each
Two double half loop antennae in end-cells	1 MW- each
Transmitter operating voltage	10 - 30 KV
Central-cell magnetic field	0.24 T
End-cell magnetic field	0.6 T
Mirror field	1.2 T
Mirror ratio	2.0
Superconductor	NbTi or high temp. S.C.

The basic superconducting tandem mirror geometry has been modified to exploit the inherent axial

asymmetry of these devices in order to provide a preferred flow direction. This approach is used to guide, control, and radially confine the plasma from injection to exhaust. The tandem mirror also ensures magnetohydrodynamic stable operation over a wide range of plasma temperatures and densities. Additionally, the mirror enables exhaust Isp and flow-rate control through manipulation of the end-cells as both input and output controlling gates.

Experimental and theoretical investigations of this propulsion concept have been carried out over several years.[12, 13, 14] Based on these results, a 10MW nuclear electric system operating at 68% efficiency has been considered. In terms of specific power or "Alpha," a value of 6 Kg/KW has been assessed.[15] This value, although somewhat optimistic, reflects brisk progress in nuclear electric technology, as well as the high-voltage (low current) characteristic of RF-heated propulsion. The expected rocket performance parameters are shown in Fig. 2.

4. Mission Concept

The mission approach considered here is the familiar "split-sprint" scenario envisioned in numerous previous studies. A one-way, slow, high-payload capacity, automated cargo ship leaves first and places a habitat, fuel, and supplies on Mars. Some of the infrastructure will be located at strategic points on orbit and on the planet's surface (an operating nuclear power plant on the surface, fuel and redundant landers on Mars orbit). Additionally, a fuel supply will be located on orbit at the edge of the Earth's gravitational sphere of influence.

2
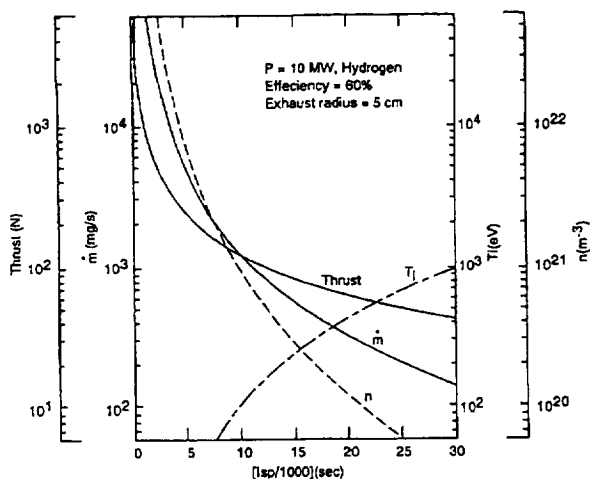
Figure 2. Theoretical rocket performance envelope for hydrogen propellant at 10 MWe and 60% efficiency.

Following completion of this robotic mission, a smaller, low-payload, fast ship will carry the crew to Mars. The ship will pick up its final fuel load for Mars at a staging rendezvous point at the edge of the Earth's sphere of influence. Failure to do so will abort the mission back to Earth. The fast cruise to Mars will be under modulated exhaust at maximum power on a trajectory designed for Mars-orbit insertion. Rendezvous with supplies and lander at Mars will be required to effect a landing.

An important feature of a human mission should be its abort capability. Failure of a major system while en route could require return to Earth or, in some cases, use of the destination planet as a "safe haven." Such abort capability was inherent (and used) in project Apollo and exists today in all Space Shuttle missions. Accordingly, interplanetary human missions should also possess such capability.

Finally, as shown in section 6, the relative motion of Earth and Mars poses an interesting challenge to the mission designer. Very fast human opposition-class (opposition is defined here as the opposite alignment of the Sun and Mars with respect to an observer situated on Earth) missions are possible with exhaust modulation; however, a symmetric return leg cannot be accomplished in the same Martian year for transit times of less than 104 days. Symmetric outbound and inbound missions of 90 days (and possibly less) one-way are possible if the crew "winters down" on Mars for a period of 2 earth years.

Such scenarios, while far too ambitious for the first mission, are not implausible for future expeditions building up to a permanent outpost on the planet. The use of Martian raw materials and installation of

abundant surface nuclear power will more than enable these long stays.

5. Mission Analysis

The power-limited equations for the interplanetary vehicle will be described here briefly. More detailed descriptions are provided by Irving and Melbourne.[16]

The thrust, "T," the power in the thrust beam, "p," the specific mass of the power plant, "α," and the thrust acceleration, "a_T," for power-limited systems are written,

$$T = \dot{m}_p \cdot c$$

$$p = \frac{1}{2} \cdot \dot{m}_p \cdot c^2$$

$$\alpha = \frac{m_W}{P} \tag{1}$$

$$a_T = \frac{-\dot{m}_p c}{m}$$

$$P = \frac{p}{\varepsilon}$$

where $\dot{m}_p$ is the propellant flow rate and c is the exhaust velocity. This quantity is related to the specific impulse "Isp" through the familiar relation: $c = g.$Isp, where g is the acceleration of gravity at the Earth's surface, 9.8 m/sec². The remaining quantities are the total spacecraft mass, "m," the power plant mass, "m_W," and its power rating, "P."

A rocket equation for power-limited propulsion systems can be written from the above equations by solving for "$(a_T)^2$" and then integrating over time as follows:

$$\frac{1}{m(t)} = \frac{1}{m_0} + \frac{\alpha}{2 \cdot m_W \cdot \varepsilon} \cdot \int_{t_o}^{t} a_T^2 \cdot dt \tag{2}$$

where "$m(t)$" is the spacecraft mass at time, "t," "m_0" is the initial spacecraft mass, and "ε" is the power plant efficiency.

The vehicle parameters can be separated from the trajectory parameters and the rocket equation can be rewritten as:

$$\frac{1}{m(t)} = \frac{1}{m_0} + \frac{1}{m_W} \cdot \beta(t)^2 \tag{3}$$

where

$$\beta(t)^2 = \frac{\alpha}{2 \cdot \varepsilon} \cdot \int_{t_o}^{t} a_T^2 \cdot dt$$

3

At the final time, "t_f," "β" can be written as,

$$[\beta(t_f)]^2 = \frac{\alpha}{\varepsilon} \cdot J^2, \text{ where:}$$

$$J^2 = \frac{1}{2} \cdot \int_{t_0}^{t_f} a_T^2 \cdot dt$$

is the performance index.

The trajectory is optimized independently of the vehicle by minimizing J^2, which effectively minimizes the amount of propellant required for the mission. This optimized trajectory is then used with the vehicle parameters, which are determined by the mission planner, to calculate the power plant and payload mass fractions.

The spacecraft mass at any time, "t," is equal to the sum of the payload mass, "m_L," the power plant mass, "m_W," and the propellant mass, "$m_p(t)$."

$$m(t) = m_L + m_W + m_p(t) \tag{4}$$

The initial propellant mass, "$m_p(0)$," is assumed to be exactly the amount of propellant necessary to complete the mission, so at the end of the mission, $m_p(t_f) = 0$.

From reference 16, the maximum payload mass fraction and the propellant mass fraction can be shown to be,

$$\left.\frac{m_L}{m_0}\right|_{maximum} = (1 - \beta)^2 \tag{5}$$

$$\frac{m_p(0)}{m_0} = \beta \tag{6}$$

where

$$\beta = \sqrt{\frac{\alpha}{\varepsilon}} \cdot J \tag{7}$$

Another parameter of interest is the Isp time history of the optimized transfer. Isp(t) is a function of the thrust acceleration time history, the integral of the thrust acceleration squared, α, ε, and J.

$$I_{sp}(t) = \frac{1}{g \cdot a_T(t)} \cdot \left[2 \cdot J \left(\sqrt{\frac{\varepsilon}{a}} - J \right) + \int_{t_0}^{t} a_T^2 \cdot dt \right] \tag{8}$$

To compute the optimal Isp as a function of time, the optimal control functions "a_{T_x}," "a_{T_y}," "a_{T_z}," and the resulting value for "J" need to be found. The functions "a_{T_x}," "a_{T_y}," and "a_{T_z}" are found by solving an optimization problem defined as follows.

The performance function is,

$$J^2 = \frac{1}{2} \int_{t_0}^{t_f} (\bar{a}_T \cdot \bar{a}_T) \cdot dt \tag{9}$$

The equations of motion are:

$$\dot{\bar{r}} = \bar{v}$$

$$\dot{\bar{v}} = -\frac{\mu \cdot \bar{r}}{r^3} + \bar{a}_T \tag{10}$$

where μ is the Sun's gravitational parameter, $1.32715 \; 10^{20}$ m³/sec².

The initial conditions are:

$$\bar{r}_0 = \bar{r}_e(t_0),$$

$$\bar{v}_0 = \bar{v}_e(t_0) \tag{11}$$

where $\bar{r}_e$ and $\bar{v}_e$ are the position and velocity vectors of the Earth at the initial time, t_0. The final

$$\bar{r}_f = \bar{r}_m(t_f)$$

$$\bar{v}_f = \bar{v}_m(t_f) \tag{12}$$

conditions are:

where $\bar{r}_m$ and $\bar{v}_m$ are the position and velocity vectors of Mars at time, t_f.

From the calculus of variations, as shown in Bryson and Ho,[17] the Hamiltonian is defined as

$$H = \sum_{i=1}^{6} \lambda_i \cdot f_i + L \tag{13}$$

where $L = \frac{1}{2}a_T^{\ 2}$ from equation (9), "f_i" are the right-hand side of equation (10), and "λ_i" are the Lagrange multipliers corresponding to equation (10).

From the first necessary conditions for an extremal,

$$\dot{\lambda}_x = -\frac{\mu}{r^3} \cdot \left[\frac{3x \cdot \left(\overline{\lambda}_v \cdot \overline{r} \right)}{r^2} - \lambda_x \right]$$

$$\dot{\lambda}_y = -\frac{\mu}{r^3} \cdot \left[\frac{3y \cdot \left(\overline{\lambda}_v \cdot \overline{r} \right)}{r^2} - \lambda_y \right]$$

$$\dot{\lambda}_z = -\frac{\mu}{r^3} \cdot \left[\frac{3z \cdot \left(\overline{\lambda}_v \cdot \overline{r} \right)}{r^2} - \lambda_z \right]$$

(14)

$$\dot{\lambda}_{\dot{x}} = -\lambda_x$$

$$\dot{\lambda}_{\dot{y}} = -\lambda_y$$

$$\dot{\lambda}_{\dot{z}} = -\lambda_z$$

where,

$$\overline{\lambda}_v = \left(\lambda_{\dot{x}}, \lambda_{\dot{y}}, \lambda_{\dot{z}} \right)$$

and

$$a_{T_x} = -\lambda_{\dot{x}}$$

$$a_{T_y} = -\lambda_{\dot{y}}$$

(15)

$$a_{T_z} = -\lambda_{\dot{z}}$$

After application of the calculus of variations, the optimization problem requires minimizing "J" as a function of the initial values of the Lagrange multipliers,

$$\lambda_x(0), \lambda_y(0), \lambda_z(0)$$

$$\lambda_{\dot{x}}(0), \lambda_{\dot{y}}(0), \lambda_{\dot{z}}(0)$$

(16)

the final time, "t_f," and satisfying the terminal constraints in equation (12).

This constrained minimization problem is solved using a numerical optimization method in the program Hybrid Optimization Technique (HOT). HOT provides the interplanetary simulation by integrating equations (10) and (14), numerically using equation (15) for the control values, and using equations (11) and (16) for the initial state and multiplier conditions, respectively. The initial λ's are iterated upon using the Davidon-Fletcher-Powell Penalty Function Method,[18] which also resides in HOT.

6. Performance

A representative set of mission scenarios, as described in section 4, was studied using the numerical techniques outlined above. No attempt has been made in this initial study to account for the gravitational effects of the departure and destination planets. Rather, the ships move in heliocentric space only under the gravity of the Sun. Boundary conditions require zero relative velocities between the ship and the planet at both the departure and arrival points. Furthermore, these points are chosen to coincide with the position of the appriopriate planet at the departure and arrival times. Optimized trajectories accounting for the planets' gravitational fields and low orbit departure and arrival, as well as assorted techniques for aerobraking and gravity assist will be taken up in a future study.

Given the launch date and the desired length of the trip, the initial state vector of Earth and the final state vector of Mars (or vice versa) are calculated. From these boundary conditions, the optimization program computes the value of "J" which, roughly described, is a measure of the fuel necessary to accomplish the given mission. From the above formulation, the assumed values of "α" and "ϵ" are used to calculate the value of "β," the propellant mass fraction of the rocket. From "β," the payload and power plant mass fractions are also calculated. The trajectory is computed considering only the heliocentric sphere of influence, and seeks to match perfectly the initial and final state vectors of the planets.

A 90-day trajectory profile from Earth to Mars (Fig. 3) will be used to illustrate the performance and properties of an exhaust-modulated rocket. The trajectories are integrated in convenient half-day (43,200 seconds) segments. Vehicle moves in heliocentric space matching the initial and final positions and velocities of Earth and Mars, respectively. Vehicle starts with zero Earth-relative velocity and arrives at Mars with zero relative velocity as well. Techniques to optimize Earth escape and Mars capture are considered separately.

5
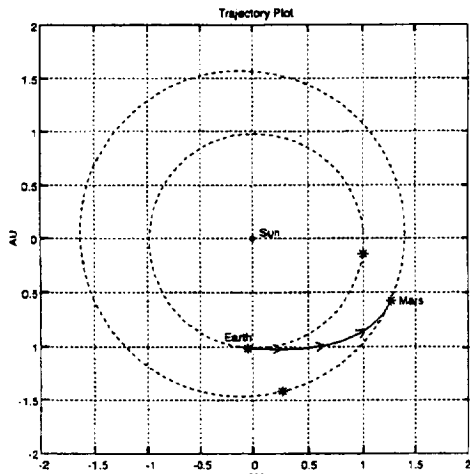
**Figure 3. Typical one-way 90-day Mars transit with exhaust modulation.**

The thrust acceleration vectors associated with the 90-day trajectory are shown in Fig. 4, while the Isp as a function of time is plotted in Fig. 5. Inspection of these graphs shows the greatest velocity changes near the beginning and the end of the mission. The midcourse phase of the trajectory is a high Isp, low-thrust "quasicoast" period. The vehicle mass variation as a function of time is shown in Fig. 6. It indicates the greatest fuel expenditure at the beginning and at the end of the trajectory.
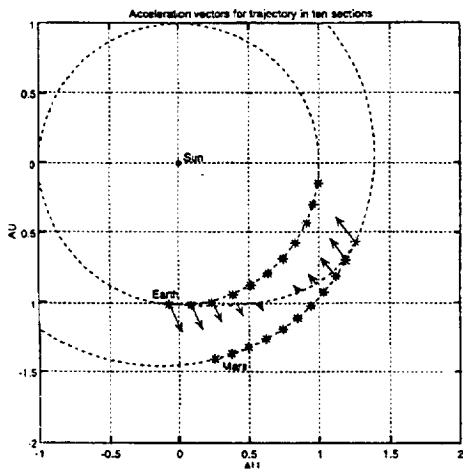

Figure 4. Trajectory plot for a 90-day transit showing the thrust acceleration vectors at 10 intervals during the mission. Thrust acceleration is nearly radial, decreasing in magnitude toward the midpoint of the mission, reversing direction, and increasing again at Mars arrival.

The eccentricity of Mars' orbit (.0934) causes a considerable variability in the radial distance an Earth-Mars trajectory must cover. The Earth's orbit, being much less eccentric (.0167), is less of a factor when determining optimal trajectories. The greater

the radial distance, the more the rocket must struggle against the gravity well of the Sun. Therefore, the best possible one-way trajectories arrive at Mars, or are launched from Mars, when the planet itself is near perihelion. This is shown in Fig. 7.
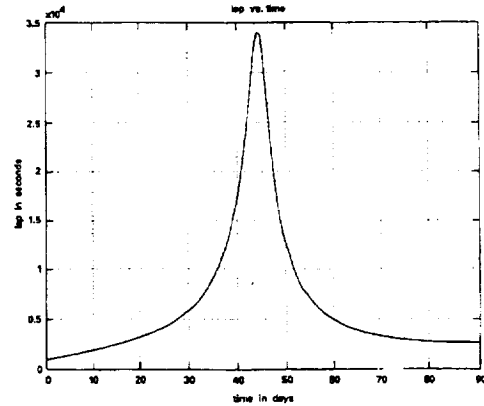

Figure 5. Isp profile over the entire transit. Isp and thrust are exchanged continuously at constant (maximum) power. The profile is nearly symmetric showing only a minor difference at Mars, due to the combined effects of a lower Sun's gravity and reduced total mass at arrival.
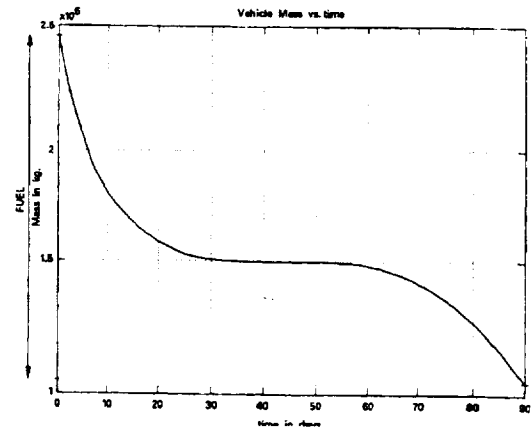
Figure 6. Total fuel expenditure. Most of the fuel is spent during the initial and final high-thrust phases of the mission. The use of gravity assist and aerobraking techniques may further reduce the fuel expenditure at these two ends.

One can define a phase angle ϑ for the transit as the angle subtended between two radii originating at the Sun and intercepting the departure and arrival points. Trajectories which traverse small phase angles are generally fuel-inefficient, as confirmed by experimentation with these approaches. A phase angle of roughly 60° yields the optimum results for a 90-day mission. Phase angles more or less than the optimum values, as determined through iterative runs, are fuel-inefficient. Thrust is wasted to counteract components of the initial velocity which would improve, rather than hinder, the rocket's travel time to Mars.

6
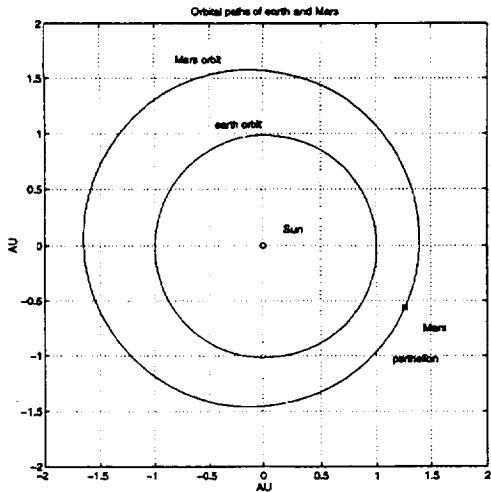
Figure 7. The eccentricity of Mars' orbit provides an optimum window of opportunity for the transit when the planet's orbit is closest to that of Earth.

The Martian year of 686.9 days forces a period of opposition of the planets approximately once every 2 years. In the years 2016 and 2018, the oppositions are relatively close to the perihelion of Mars. These 2 years offer three launching options: two human and one robotic. For example, the "tugboat" profile shown in Fig. 8 gives little regard to the travel time of the rocket and seeks to maximize the payload mass fraction placed in Mars orbit. As described in section 4, such a profile is used to deliver the habitat, return fuel, and supplies to Mars. Once on the planet, in situ resource utilization machinery could be set in motion. The nuclear power plant on board might also be used to provide supplemental power to the habitat and, hence, become part of the useful payload upon arrival.

Once the operation of the equipment is started and verified from the safety of Earth, the human mission could commence during the next 2-year cycle. The profile shown in Fig. 8 is a 180-day mission with a 66.66% payload mass fraction. However, longer missions with better mass fractions are possible.

The first human mission considered here is a short one shown in Fig. 9. This profile is executed within the same Martian year. The mission encompasses a 101-day outbound trip, a 30-day stay, and a 104-day return. This "speedboat" option is one of the shortest Mars missions thus far projected, albeit with a 2% payload mass fraction in each direction.

Such short human transits ameliorate the physiological hazards associated with long human exposure to the space environment. Moreover, the continuous acceleration provides an artificial gravity

of sorts which may have added positive effects. Reduced mission duration (235 days) would put much less of a requirement on the development of long-duration facilities and their associated maintenance. Radiation exposure would be reduced as well.
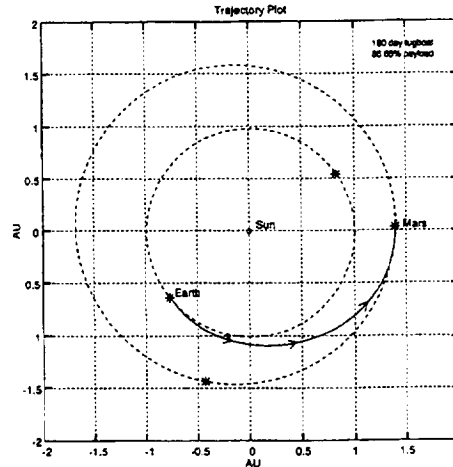
Figure 8. Typical trajectory plot for a high payload, longer duration transit. Values of 18% payload-mass fraction and 90 days are also possible with the same engine, illustrating the dual nature of this propulsion system.
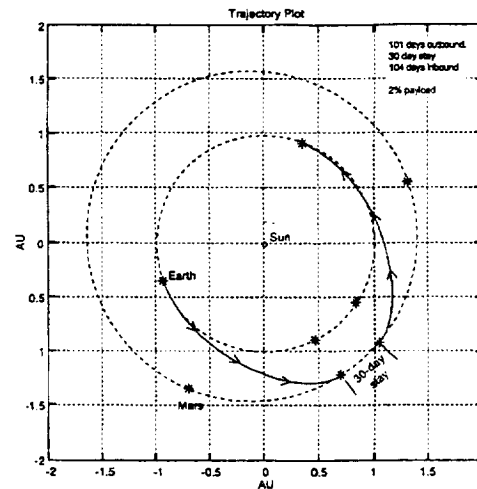

Figure 9. A total mission with nearly symmetric inbound and outbound legs. While shorter transits are allowed by the propulsion system, the planet's alignment becomes unfavorable for transits less than 100 days. Shorter transits are possible if the mission includes an extended stay on the surface of the planet.

Reducing the time of stay on Mars in this profile does not yield substantial improvements in the transit times or payload mass fractions. Shortening the stay to 20 days might yield a decrease of 6 days outbound and 5 days inbound and keep the payload mass fraction constant.

7

7. Abort Scenarios

An important attribute of the exhaust-modulated plasma rocket is its powered abort capability. Should the habitat fail, the crew become incapacitated, or one or more of the modules of the rocket cluster fail, the system has a limited capability to return directly to Earth or abort to Mars, albeit with an increased travel time.

The issues associated with powered aborts back to Earth are the nominal mission profile, the time of abort, and the abort duration. Given the nominal mission profile and the time at which the decision to abort is implemented, the fuel remaining and the initial state vector of the spacecraft are determined. The abort duration specifies the location of Earth at the arrival point and, consequently, the final state vector. The same optimization program is then used to determine the necessary mass fractions to accomplish such an abort. Comparing the mass fractions of the vehicle at the time of abort and the mass fractions necessary to accomplish the abort, it is then possible to determine whether the desired abort is feasible.
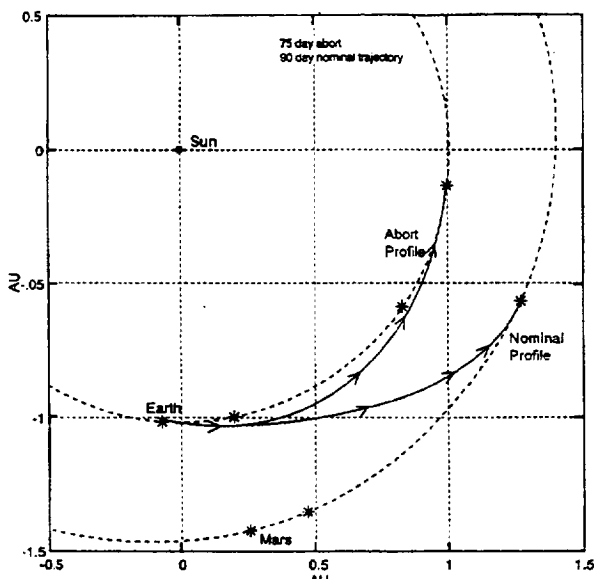

Figure 10. Typical powered abort returning the spacecraft to Earth 75 days after abort condition is declared. Such abort windows exist within 15 to 20 days after Earth escape. The scenario depicted here assumes a full-up propulsion system after the abort is declared.

The abort scenarios considered here are shown in Figs. 10 and 11. They occur 15 days into the 90-day mission, and last 75 and 180 days, respectively. Both are possible; however, the 180-day return can make it back with fuel to spare, as in a propellant system failure. Conversely, if the fuel is available, this demonstrates the possibility of aborts even after 15

days en route. In these cases, the velocity away from Earth orbit and the fuel remaining are the driving factors. In general, the efficiency of fuel usage increases with the abort duration. While the calculations suggest the possibility of powered aborts due to a partial engine cluster failure, these have not yet been simulated.

The three scenarios depicted above embody the fundamental operational requirements for a human mission to the planet Mars.
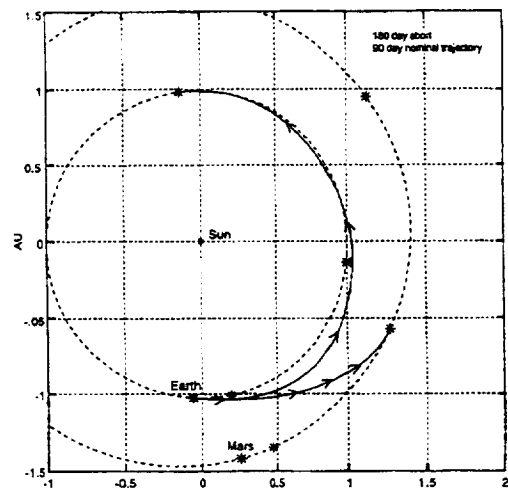
Figure 11. Typical 180-day abort trajectory. This longer return patch would result from a propellant system failure reducing the fuel available and hence increasing the return time. Abort windows exist within 15 to 20 days from Earth escape.
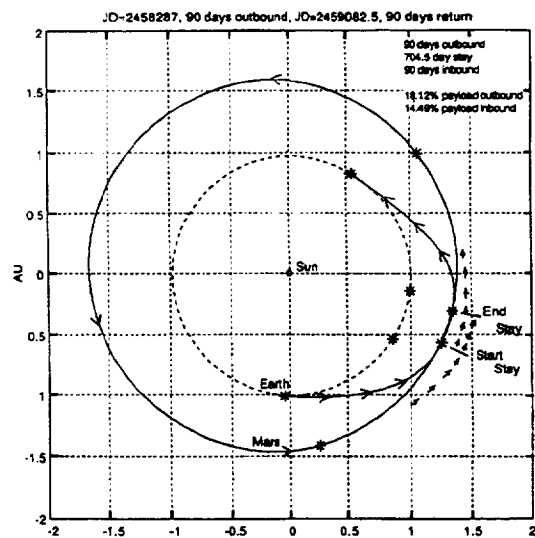
Figure 12. Complete extended-duration mission with symmetric inbound and outbound legs. Payload-mass fractions are considerably higher with this option, due to the optimum alignment of the planets.

8. Extended-Stay Missions

Finally, the extended-stay Mars mission is considered. The complete profile is shown in Fig. 12. The 90-day outbound trip is launched during the optimum point in an initial Martian year. This choice increases the payload mass to 18.12%. After a 704.5-day stay, the craft returns in 90 days with a 14.49% payload-mass fraction. The short transit times minimize radiation exposure in space, assuming improved shielding of the Martian habitat. The improved payload-mass fractions are possible because of the 2-year wait for the next opposition of Earth and Mars near Mars' perihelion.

Such a long-stay mission would require refinements in closed-environment recycling techniques, supplemented by extensive in situ resource utilization. However, the benefits gained are payload mass fractions 7 to 9 times better than those offered in the 30-day stay mission profile. Perhaps this would be the choice profile for a second, longer duration mission to Mars, once the lessons from the first have been absorbed.

The trajectories examined have not accounted for potential improvements in performance, such as aerobraking, gravity assist, and capture into a highly elliptical orbit. Currently, use of the "crew taxi" concept is assumed. The crew would be flown out to the main vehicle once it had approached escape velocity. However, given its high-thrust capability, further consideration of the performance of the rocket in Earth's and Mars' spheres of influence is planned.

9. Conclusion

For power-limited rockets, the technique of exhaust modulation at constant power provides the optimum approach to fast interplanetary missions. A "split-sprint" mission scenario can be accomplished with a one-way, 180-day robotic space-tug precursor mission, followed by a 101-day, low-payload, human fast boat. After a 30-day stay, the human ship can return to Earth in 104 days. For a long-stay mission, the transit times can be considerably shorter and the payload-mass fraction increased. This modality may be utilized when a permanent habitat is in place.

Such exhaust-modulated plasma rockets have now reached the experimental stage and have become increasingly attractive as a result of recent developments in ion cyclotron plasma heating techniques and superconducting magnetic confinement and vectoring systems. Furthermore, these engines provide high-thrust orbital maneuvering capability and abort margins which are essential for human missions to the planet Mars and beyond.

10. References

[1] Duke, M., et al., "EXPO Mars Program Study," NASA Exploration Programs Office, presentation to the Associate Administrator for Exploration, October 9, 1992.

[2] Doherty, M.P. and Holcomb, R.S., "Summary and Recommendations on Nuclear Electric Propulsion Technology for the Space Exploration Initiative," NASA Technical Memorandum 105707, April 1993.

[3] Hack, K.J., et al., "Evolutionary Use of Nuclear Electric Propulsion," AIAA Space Programs and Technologies Conference, Huntsville, Ala., AIAA 90-3821, NASA Lewis Research Center, September 1990.

[4] Chang-Díaz, F.R. and Yang, T.F., "Design Characteristics of the Variable Isp Plasma Rocket," AIAA, 22nd International Electric Propulsion Conference, IEPC-91-128, October 1991.

[5] Irving, J.H. and Blum, E.K., "Comparative Performance of Ballistic and Low-Thrust Vehicles for Flight to Mars," *Vistas In Astronautics*, Vol. II, Pergamon Press, New York, 1959.

[6] Stuhlinger, E., *Ion Propulsion for Space Flight*, McGraw-Hill, 1964.

[7] Chang, F.R., "The Hybrid Plume Plasma Rocket," NASA Johnson Space Center Internal Report, January 1982.

[8] Chang, F.R. and Fisher, J.L., "A Supersonic Gas Target for a Bundle Divertor Plasma," *Nuclear Fusion*, Vol. 22, 1982.

[9] Chang-Díaz, F.R., et al., "A Tandem Mirror Hybrid Plume Plasma Propulsion Facility," 20th International Electric Propulsion Conference, West Germany, IEPC-88-126; October 1988.

[10] Chang-Díaz, F.R. and Yang, T.F., "Tunable Plasma Rockets with RF-Heating and Superconducting Thrust Chambers," Research and Development Annual Report, NASA Technical Memorandum 104777, 1992.

[11] Baldwin, D.E. and Logan, B.G., "TMX Major Project Proposal," Lawrence Livermore National Laboratory Report, 11-Prop-148 (1977).

[12] Krueger, W.A., "Plasma and Neutral Jet Interactions in the Exhaust of a Magnetic

Confinement System," Ph.D. Thesis,
Massachusetts Institute of Technology, June 1990.

[13]Peng, S., "ICRF Wave Propagation and Plasma
Coupling Efficiency in a Linear Magnetic Mirror,"
Ph.D. Thesis, Massachusetts Institute of
Technology, 1991.

[14]Yang, T.F., et al., "ICRH Plasma Heating in the
Tandem Mirror Rocket," AIAA-91-2338, 27th
Joint Propulsion Conference, Sacramento, Cal.,
June 1991.

[15]"Ultrahigh Power Space Nuclear Power System
Design and Development," Rocketdyne Division
Report, 1990.

[16]Melbourne, W.G., "Interplanetary Trajectories and
Payload Capabilities of Advanced Propulsion
Vehicles," NASA Jet Propulsion Laboratory
Report 32-68, Pasadena, Cal., March 31, 1961.

[17]Bryson, A.E., Jr. and Ho, Yu-Chi, *Applied Optimal
Control, Optimization, Estimation, and Control*,
Hemisphere Publishing Corporation, Washington,
D.C., 1975.

[18]Johnson, I.L., Jr., "The Davidon-Fletcher-Powell
Penalty Function Method: A Generalized Iterative
Technique for Solving Parameter Optimization
Problems," NASA Technical Note D-8251,
Johnson Space Center, May 1976.

REPORT DOCUMENTATION PAGE

1. AGENCY USE ONLY (Leave Blank)	2. REPORT DATE March 1995	3. REPORT TYPE AND DATES COVERED NASA Technical Paper

4. TITLE AND SUBTITLE

Rapid Mars Transits With Exhaust-Modulated Plasma Propulsion

5. FUNDING NUMBERS

6. AUTHOR(S)

Franklin R. Chang Diaz, Michael M. Hsu*, Ellen Braden, Ivan Johnson, Tien Fang Yang**

7. PERFORMING ORGANIZATION NAME(S) AND ADDRESS(ES)

Lyndon B. Johnson Space Center
Houston, TX 77058

8. PERFORMING ORGANIZATION REPORT NUMBERS

S-795

9. SPONSORING/MONITORING AGENCY NAME(S) AND ADDRESS(ES)

National Aeronautics and Space Administration
Washington, D.C. 20546-0001

10. SPONSORING/MONITORING AGENCY REPORT NUMBER

TP-3539

11. SUPPLEMENTARY NOTES

*US Navy det Dept of Physics, Cambridge University, U.K.
**Yang Technologies, Inc., Cambridge, MA

12a. DISTRIBUTION/AVAILABILITY STATEMENT
Unclassified/Unlimited
Available from the NASA Center for AeroSpace Information
800 Elkridge Landing Road
Linthicum Heights, MD 21090-2934
(301) 621-0390   Subject Category: 20

12b. DISTRIBUTION CODE

13. ABSTRACT *(Maximum 200 words)*

The operational characteristics of the Exhaust-Modulated Plasma Rocket are described. Four basic human and robotic mission scenarios to Mars are analyzed using numerical optimization techniques at variable specific impulse and constant power. The device is well suited for "split-sprint" missions, allowing fast, one-way low-payload human transits of 90 to 104 days, as well as slower, 180-day, high-payload robotic precursor flights. Abort capabilities, essential for human missions, are also explored.

14. SUBJECT TERMS

robotic missions, Mars missions, specific impulse, constant power, plasma propulsion, trajectory optimization, Mars probes, propulsion system performance

15. NUMBER OF PAGES
14

16. PRICE CODE

17. SECURITY CLASSIFICATION OF REPORT	18. SECURITY CLASSIFICATION OF THIS PAGE	19. SECURITY CLASSIFICATION OF ABSTRACT	20. LIMITATION OF ABSTRACT
Unclassified	Unclassified	Unclassified	